FEBS Letters 584 (2010) 2397–2402

FEBS Letters
journal homepage: www.FEBSLetters.org

Hexokinase inhibits flux of fluorescently labeled ATP through mitochondrial outer membrane porin

Irina V. Perevoshchikova, Savva D. Zorov, Elena A. Kotova, Dmitry B. Zorov, Yuri N. Antonenko *

Belozersky Institute of Physico-Chemical Biology, Department of Bioengineering and Bioinformatics, Moscow State University, Moscow 119991, Russia

ARTICLE INFO

Article history:
Received 10 February 2010
Revised 13 April 2010
Accepted 13 April 2010
Available online 22 April 2010

Edited by Peter Brzezinski

Keywords:
Mitochondria
Voltage dependent anion channel
Hexokinase
Fluorescence correlation spectroscopy

ABSTRACT

Mitochondrial function requires maintaining metabolite fluxes across the mitochondrial outer membrane, which is mediated primarily by the voltage dependent anion channel (VDAC). We applied fluorescence correlation spectroscopy (FCS) to study regulation of the VDAC functional state by monitoring distribution of fluorescently labeled ATP (BODIPY-FL-ATP) in isolated intact rat liver and heart mitochondria. Addition of mitochondria to BODIPY-FL-ATP solution resulted in accumulation of the fluorescent probe in these organelles. The addition of hexokinase II (HKII) isolated from rat heart led to a decrease in the BODIPY-FL-ATP accumulation, while a 15-residue peptide corresponding to the N-terminal domain of hexokinase did not produce this effect. Therefore, the hexokinase-induced inhibition of the ATP flow mediated by VDAC was revealed in isolated mitochondria.

1. Introduction

The common pathway for the translocation of metabolites through the mitochondrial outer membrane is the voltage dependent anion channel (VDAC) channel [1,2], having β-barrel structure similarly to bacterial porins [3–5]. VDAC has been shown to mediate the flow of ATP [6,7] when reconstituted into lipid bilayers. By interacting with VDAC, different mitochondrial and cytosolic proteins modulate its transport activity [8,9]. In particular, the type I and type II isozymes of hexokinase coexisting in cardiac and skeletal muscles [10] have high affinity for VDAC [11–13], which may regulate the ratio between oxidative phosphorylation and glycolytic pathways in cells [14,15]. A correlation was observed between association of hexokinase with mitochondria and incidence of apoptotic cell death – the higher the association, the less the probability of cell death [16,17]. Although with bilayer-reconstituted VDAC, hexokinase I was shown to promote the closed state of the channel [18,19], the effect of hexokinase on the transport activity of VDAC, in particular, on the ATP flux through this channel in isolated mitochondria has not been determined so far.

In the present work, we used ATP labeled with the fluorescent marker BODIPY conjugated to the ribose ring via the 2′-(or-3′)-position (BODIPY-FL-ATP) for evaluating the transport activity of VDAC in rat liver mitochondria. BODIPY-FL-ATP has previously been employed for characterization of ATP-binding sites in vacuolar ATPase [20]. The accumulation of BODIPY-FL-ATP in mitochondria was measured by fluorescence correlation spectroscopy (FCS) which is known to be a powerful and convenient tool for determining mobility of target molecules both in cells and in a suspension of subcellular structures [21,22]. FCS enables to detect fluorescence at a single molecule level from a very small volume ($\sim 10^{-15}$ l) with microsecond resolution. Recently, the modified FCS method (we coined it the peak intensity analysis (PIA)) was applied to measure tetramethylrhodamine ethyl ether (TMRE) potential-sensitive accumulation in mitochondria, which allowed to estimate the number of mitochondrial particles and the magnitude of mitochondrial membrane potential with high accuracy [23]. In the present study we demonstrate that with BODIPY-FL-ATP, PIA enables to evaluate the transport activity of VDAC, in particular, the ATP flux through this channel. The binding of hexokinase to VDAC, similarly to that of Koenig's polyanion, led to inhibition of the flux of labeled ATP into mitochondria.

2. Materials and methods

2.1. Materials

Most chemicals were from Sigma; succinate and sucrose were from ICN. Rhodamine 6G was from Fluka. BODIPY-FL-ATP

Abbreviations: FCS, fluorescence correlation spectroscopy; HKII, hexokinase II; VDAC, voltage dependent anion channel; BODIPY-FL-ATP, BODIPY® FL 2′-(or-3′)-O-(N-(2-aminoethyl) urethane) adenosine 5′-triphosphate; BODIPY-FL-ADP, BODIPY® FL 2′-(or-3′)-O-(N-(2-aminoethyl) urethane) adenosine 5′-diphosphate

* Corresponding author. Fax: +70 95 9393181.
E-mail address: antonen@genebee.msu.ru (Y.N. Antonenko).

0014-5793/$36.00
doi:10.1016/j.febslet.2010.04.033

(BODIPY® FL 2′-(or-3′)-O-(N-(2-aminoethyl) urethane) adenosine 5′-triphosphate) and BODIPY-FL-ADP (BODIPY® FL 2′-(or-3′)-O-(N-(2-aminoethyl) urethane) adenosine 5′-diphosphate) were from Molecular Probes. The peptide MIASHLLAYFFTELN-amide corresponding to the N-terminus of hexokinase was synthesized by the solid phase method on 2-chloro-trityl-chloride polystyrene resin using the standard Fmoc chemistry procedure with HOBt/DIC carboxylic groups activation in a Syro I peptide synthesizer (Muti-SynTech, Germany) by Nataliya Egorova at Shemyakin-Ovchinnikov Institute of Bioorganic Chemistry (Russia). To achieve peptide cleavage and deprotection, the peptide resins were treated with trifluoroacetic acid–ethandithiol–triisopropylsilane–water (94: 2.5:1:2.5) for 2.5 h. Peptides were purified by preparative RP-HPLC on a C16 column (BioChemMack, Russia) with acetonitryl gradient in 0.1% trifluoroacetic acid in water and characterized by analytical HPLC and matrix-assisted laser desorption ionization time-of-flight (MALDI-TOF) mass-spectroscopy. Finally the peptide was dissolved in methanol. Koenig's polyanion was synthesized by Nikolay Melik-Nubarov at the Moscow State University (Russia).

2.2. FCS experimental setup

The home-made setup was described previously in [23]. Briefly, fluorescence excitation and detection utilized a Nd:YAG solid state laser with a 532-nm beam attached to an Olympus IMT-2 epifluorescent inverted microscope equipped with a 40×, NA 1.2 water immersion objective (Carl Zeiss, Jena, Germany). The fluorescence light passed through an appropriate dichroic beam splitter and a long-pass filter and was imaged onto a 50-μm core fiber coupled to an avalanche photodiode (SPCM-AQR-13-FC, Perkin–Elmer Optoelectronics, Vaudreuil, Quebec, Canada). The signal from an output was sent to a personal computer using a fast interface card (Flex02-01D/C, Correlator.com, Bridgewater, NJ). The data acquisition time was 30 s. The fluorescence was recorded from the confocal volume located at about 50 μm above the coverslip surface with 50 μl of the buffer solution added. Most of the data were collected under the conditions of stirring a suspension by a paddle-shaped 3-mm plastic bar rotated at 600 rpm. To calibrate the setup, we recorded the autocorrelation function of fluorescence of a solution of Rhodamine 6G which was characterized by the correlation time τ_D estimated from Eq. (1). Assuming the diffusion coefficient of the dye to be 2.5×10^{-6} cm^2/s, the value of the confocal radius $\omega = 0.42$ μm was obtained. The correlated fluorescence emission signals were fitted to the three-dimensional autocorrelation function [24].

$$G(\tau) = 1 + \frac{1}{N}\left(\frac{1}{1+\frac{\tau}{\tau_D}}\right)\left(\frac{1}{\sqrt{1+\frac{\omega^2\tau}{z_0^2\tau_D}}}\right) \quad (1)$$

with τ_D being the characteristic correlation time during which a molecule resides in the observation volume of radius ω and length z_0, given by $\tau_D = \omega^2/4D$, where D is the diffusion coefficient, N is the mean number of fluorescent particles in the confocal volume.

2.3. Treatment of the fluorescence signal (PIA procedure)

Fluorescence traces with the sampling time of 25 μs were analyzed using WinEDR Strathclyde Electrophysiology Software designed by Dempster (University of Strathclyde, UK) or another program with an algorithm developed by van den Bogaart and colleagues [25]. The software, originally designed for the single-channel analysis of electrophysiological data, enables one to count the number of peaks ($n(F > F_0)$) of the FCS signal having amplitudes higher than the defined value (F_0).

2.4. Isolation of mitochondria

Rat liver and heart mitochondria were isolated by differential centrifugation [26] in a medium containing 250 mM sucrose, 20 mM MOPS, 1 mM EGTA, 1.2 mg/ml bovine serum albumin, pH 7.4. The final washing was performed in the same medium. Protein concentration was determined using bicinchoninic acid as described in [27]. Handling of animals and experimental procedures were conducted in accordance with the international guidelines for animal care and use and were approved by the Institutional Ethics Committee of A.N. Belozersky Institute of Physico-Chemical Biology at the Moscow State University.

2.5. Hexokinase II isolation from rat heart

Hexokinase II (HKII) was isolated according to [28] with modifications of the procedure for isolation from rat heart. Briefly, rat hearts were homogenized in 6-fold excess of isolation buffer (10 mM KH_2PO_4, 0.5 mM dithioetrethol, pH 7.4). After centrifugation at 15 000×g during 15 min a supernatant was supplemented with DEAE-cellulose prepared with 1 mM KH_2PO_4, pH 7.0 (100 mg for 1.5 U hexokinase) and incubated during 10 min. DEAE-cellulose particles were filtered by means of a Buechner fun-

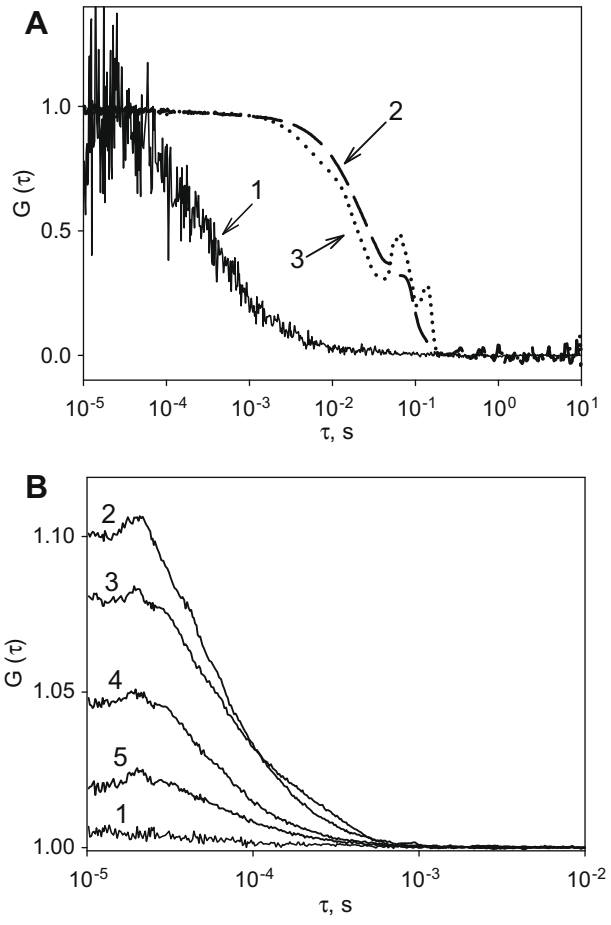

Fig. 1. (A) Normalized autocorrelation functions of 25 nM BODIPY-FL-ATP (solid curve), after the addition of rat liver mitochondria (dashed curve), and subsequent addition of 1 mM ATP (dotted curve). (B) Autocorrelation functions of 25 nM BODIPY-FL-ATP (curve 1), after the addition of rat liver mitochondria (curve 2), and subsequent addition of increasing concentrations of ATP (curve 3–10 μM, curve 4–100 μM, curve 5–1 mM) measured under stirring conditions. The solution was 0.25 M sucrose, 20 mM MOPS, 1 mM EGTA, pH 7.4. The concentration of mitochondrial protein was 0.083 mg/ml.

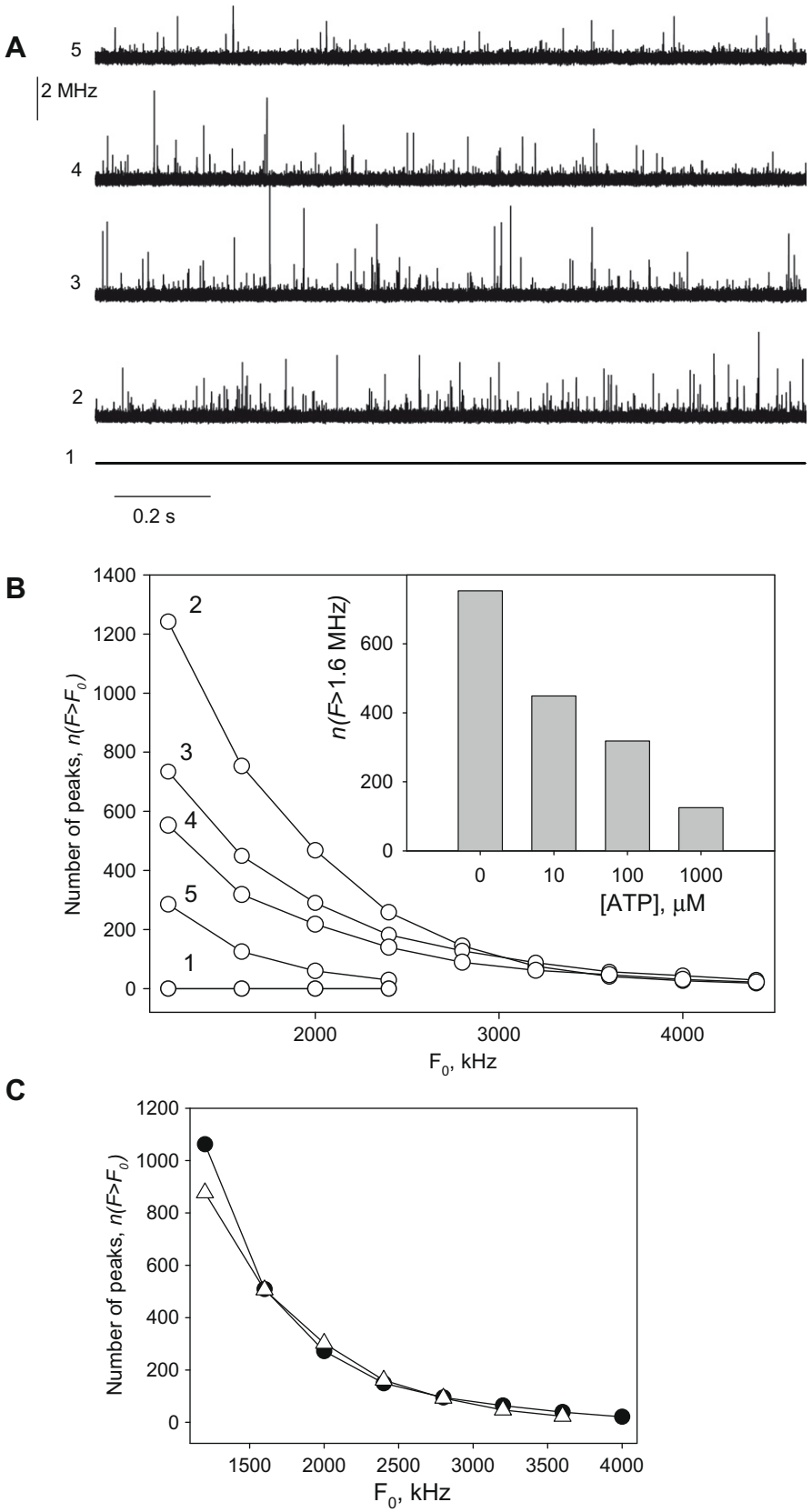

Fig. 2. (A) Time-resolved count rates of 25 nM BODIPY-FL-ATP in the absence (curve 1) and in the presence (curve 2) of rat liver mitochondria (0.083 mg/ml) in the incubation buffer, and after the subsequent additions of increasing concentrations (10 μM, 100 μM, 1 mM) of ATP (curves 3–5). The signal was recorded under stirring condition in solution: 250 mM sucrose, 20 mM MOPS, 1 mM EGTA, pH 7.4. (B) Corresponding dependences of $n(F > F_0)$ on F_0 (circles) for 25 nM BODIPY-FL-ATP. Insert: the dependence of the number of peaks with the intensity exceeding 1.6 MHz on ATP concentration. (C) The dependence of $n(F > F_0)$ on F_0 for 25 nM BODIPY-FL-ADP in the presence of rat liver mitochondria (circles). Triangles – the same after the addition of 4 mM ADP.

nel, washed with the isolation buffer to remove unbound proteins, and then incubated for 10 min in the isolation buffer supplemented with 100 mM KCl. Subsequent filtration through a Buechner funnel was followed by the addition of ammonium sulfate (up to 50%) and stirring during 20 min. After centrifugation (30000×g during 20 min), the pellet was dissolved in isolation buffer containing 0.125 M KCl and dialyzed against the same solution during 3 h. Hexokinase activity was measured spectrophotometrically at room temperature at 340 nm by coupling NADPH formation to the production of glucose-6-phosphate by HKII and its oxidation by glucose-6-phosphate dehydrogenase. The reaction mixture (1 ml) contained 100 mM Tris, 130 mM NaCl, 3.5 mM $MgCl_2$, 0.15 mM $CaCl_2$ supplemented with 1 mM NADP, 10 mM glucose, 2 mM ATP, pH 8.5. A 100-fold excess of glucose-6-phosphate dehydrogenase over HKII was employed. Typical activity of HKII samples was about 1 μmol/min mg protein.

2.6. Optical measurements

Fluorescence from standard 2-ml cuvettes was recorded with a Panorama Fluorat 02 (Lumex, Russia) fluorescence spectrophotometer with excitation and emission slits adjusted to 5 nm.

3. Results and discussion

To test the ability of BODIPY-FL-ATP to interact with mitochondria, the normalized autocorrelation function of this fluorescent probe (Fig. 1A) was measured before (curve 1) and after (curve 2) the addition of mitochondria. A pronounced shift of the autocorrelation function toward larger correlation times reflected a dramatic decrease in the diffusion coefficient (D) of BODIPY-FL-ATP that occurred upon association of the dye with mitochondria. Assuming $D = 250\ \mu m^2/s$ for Rhodamine 6G, one can obtain $D = 230\ \mu m^2/s$ for free BODIPY-FL-ATP and $D = 0.8\ \mu m^2/s$ for the dye associated with mitochondria. Armbruster et al. [20] obtained $D = 220\ \mu m^2/s$ for free BODIPY-FL-ATP. The addition of unlabeled ATP did not change the normalized autocorrelation function (curve 3) which might indicate that binding of BODIPY-FL-ATP to mitochondria was unspecific. However, further experiments showed that this conclusion was premature. Fig. 1B presents non-normalized autocorrelation functions $G(\tau)$ measured under the continuous stirring conditions used in order to increase statistics of measurements of the parameter N, i.e. the number of particles. $G(\tau)$ increased upon the addition of mitochondria and decreased gradually, as the concentration of unlabeled ATP increased (Fig. 1B), thereby showing that ATP could liberate a substantial part of bound BODIPY-FL-ATP which led to an increase in the parameter $N = 1/G(\tau \to 0)$. It is noteworthy that under the stirring conditions τ_D was determined mainly by hydrodynamic parameters rather than by diffusion of BODIPY-FL-ATP.

As it has been shown in our previous work, accumulation of a fluorescent probe in mitochondria can be characterized by special treatment of the fluorescence signal measured by an FCS setup, i.e. PIA [23]. Fig. 2A shows recordings of BODIPY-FL-ATP fluorescence measured in the absence (curve 1) and in the presence (curve 2) of mitochondria, and after the subsequent additions of increasing concentrations of ATP (curves 3–5). It is seen that the number of bursts or peaks of the signal reflecting the appearance of bright mitochondrial particles in the confocal volume decreased, as the concentration of ATP increased. Therefore, BODIPY-FL-ATP and

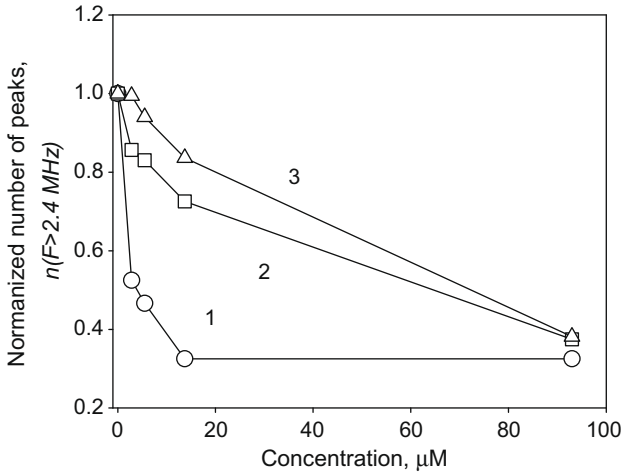

Fig. 3. Dependences of the normalized number of FCS signal peaks of Bodipy-FL-ATP with the intensity exceeding 2.4 MHz on the concentration of ATP (curve 1), GTP (curve 2) and tripolyphosphate (curve 3). The signal was recorded under stirring conditions in solution: 250 mM sucrose, 20 mM MOPS, 1 mM EGTA, pH 7.4, 0.044 mg/ml rat liver mitochondria, 25 nM Bodipy-FL-ATP, 2 μM rotenone.

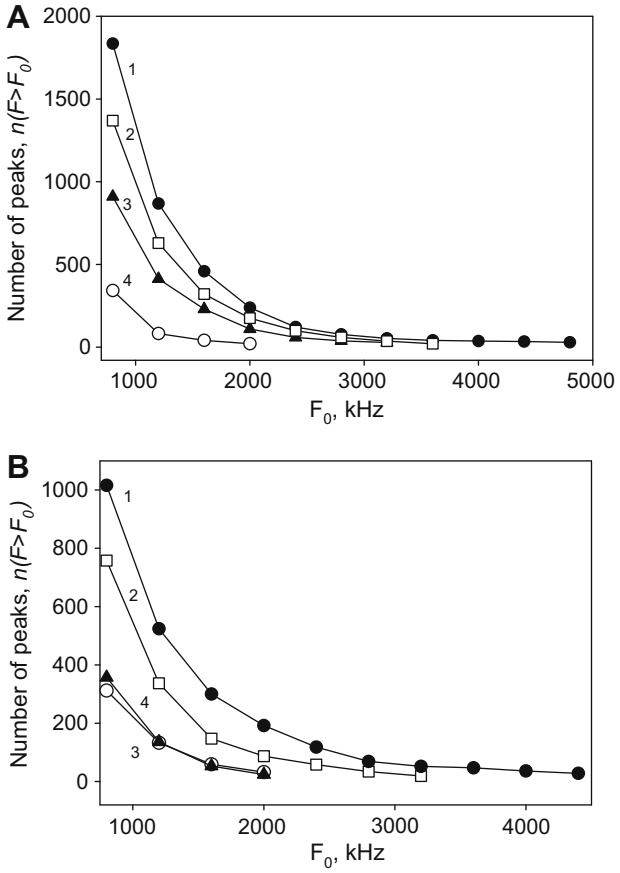

Fig. 4. (A) The effect of Koenig's polyanion and atractyloside on the plot of the number of FCS signal peaks ($n(F > F_0)$) of BODIPY-FL-ATP with amplitudes higher than the defined value (F_0) versus the F_0 value measured in mitochondrial suspension (0.044 mg/ml): (1) rat liver mitochondria supplemented with 2 μM rotenone, 25 nM BODIPY-FL-ATP; (2) mitochondria supplemented with 2 μM rotenone, 100 μM atractyloside, 25 nM BODIPY-FL-ATP; (3) mitochondria supplemented with 2 μM rotenone, 0.06 mg/ml Koenig's polyanion, 25 nM BODIPY-FL-ATP; and (4) mitochondria supplemented with 2 μM rotenone, 25 nM BODIPY-FL-ATP, 2 mM ATP. (B) The effect of NADH and NAD^+ on the plot of the number of FCS signal peaks ($n(F > F_0)$) of BODIPY-FL-ATP with amplitudes higher than the defined value (F_0) versus F_0 measured in mitochondrial suspension (0.037 mg/ml): (1) rat liver mitochondria supplemented with 2 μM rotenone, 25 nM BODIPY-FL-ATP; (2) mitochondria supplemented with 2 μM rotenone, 2 mM NAD^+, 25 nM BODIPY-FL-ATP; (3) mitochondria supplemented with 2 μM rotenone, 2 mM NADH, BODIPY-FL-ATP; and (4) mitochondria supplemented with 2 μM rotenone, 25 nM BODIPY-FL-ATP, 2 mM ATP.

ATP actually compete for binding sites in mitochondria. The accumulation of BODIPY-FL-ATP in mitochondria was slightly dependent on the presence of rotenone and on mitochondrial energization. According to the results of the PIA statistical treatment displayed in Fig. 2B, the addition of 1 mM ATP brought about a 6-fold decrease in the number of FCS signal peaks with amplitudes exceeding the value of 1.6 MHz (insert). In contrast to BODIPY-FL-ATP, the binding of BODIPY-FL-ADP apparently was unspecific, because the number of peaks obtained with this marker did not depend on the presence of ADP (Fig. 2C). Control experiments demonstrated that the addition of mitochondria to the solution of the low-molecular-weight hydrophilic fluorescent dye sulforhodamine B did not result in the appearance of FCS signal peaks which suggested the requirement of nucleotide moieties in the structure of a fluorescent probe for its accumulation in mitochondria.

Fig. 3 demonstrates the dependence of the FCS-detected BODIPY-FL-ATP accumulation in mitochondria on ATP, GTP and tripolyphosphate concentrations. Apparently, ATP is able to replace BODIPY-FL-ATP just at a few micromolar concentration, while with GTP and tripolyphosphate, one order of magnitude higher concentrations are required.

Bearing in mind that the ATP fluxes through mitochondrial outer and inner membranes are controlled by VDAC and ATP/ADP translocator, respectively [29,30], we addressed the effect of Koenig's polyanion (VDAC inhibitor) [31,32] and atractyloside (ATP/ADP translocator inhibitor) [33,34] on the accumulation of BODIPY-FL-ATP in mitochondria (Fig. 4A). An approximately 2-fold decrease in the number of FCS signal peaks with amplitudes exceeding the value of 1.6 MHz was observed, if mitochondria added to the BODIPY-FL-ATP solution were preincubated with 0.06 mg/ml Koenig's polyanion for 5 min. The effect of atractyloside was substantially less pronounced suggesting that BODIPY-FL-ATP is bound predominantly in the mitochondrial intermembrane space. It is known that this compartment contains different ATP-binding proteins such as adenylate kinase, creatine kinase and others. The nucleotide binding sites of VDAC might also be involved in the BODIPY-FL-ATP binding to mitochondria [35–37].

According to [37,38], NAD^+ and NADH can block the transport activity of VDAC, with the effect of NADH being stronger than that of NAD^+. In line with this, the inhibitory effect of NADH on the BODIPY-FL-ATP accumulation was substantially stronger compared to NAD^+ (Fig. 4B). These data support our conclusion that the accumulation of BODIPY-FL-ATP in mitochondria is determined by the activity of VDAC.

As seen from Fig. 5A, the addition of hexokinase II isolated from rat heart prevented the accumulation of BODIPY-FL-ATP in rat heart mitochondria. The supplementation of glucose-6-phosphate led to partial restoration of the FCS signal of BODIPY-FL-ATP reflecting its accumulation in mitochondria. The effect of HKII was absent, if the enzyme was inactivated by heating (5 min at 100 °C, not shown). Thus, it can be concluded that HK binding triggers a certain change in VDAC functional state that leads to reduction of the ATP flux through the porin channel.

It is generally accepted that the N-terminal region of hexokinase is involved in binding to mitochondria [39,40,18]. In our experiments, the peptide composed of the first 15 amino acid residues of hexokinase, i.e. MIASHLLAYFFTELN-amide, was unable to inhibit the accumulation of BODIPY-FL-ATP in rat heart mitochondria even at high mole concentrations (Fig. 5B). Based on this result, we speculate that the VDAC-binding and the VDAC-blocking domains of hexokinase are not identical. It is relevant to this point that according to the findings of [17], the interaction of HK with VDAC1 is mediated by multiple interaction sites.

At first glance, the conclusion about the inhibition of the VDAC-mediated ATP flux by hexokinase binding compromises the main mitochondrial function – to generate ATP and to transport it to cytosol in order to provide non-stop metabolic operation. In fact, hexokinase II capable to bind to mitochondria is abundantly present in the cytosol of a number of tissues (heart, brain) which potentially must hinder or even block the delivery of ATP to cytosolic ATP users. However, one can speculate that such process may be highly regulated and in reality such an arrest of ATP transport from mitochondria to cytosol does not take place. Apart from this, hexokinase bound to VDAC may catch released ATP to phosphorylate glucose rather than block ATP transport [41]. This process falls into a category of widely discussed metabolic channeling phenomena [42,43].

It is worth mentioning that under some pathological conditions, partial or complete arrest of VDAC functioning does occur [44]. For example, ethanol infusion to rats resulted in progressing the pathology characterized by VDAC impermeability for cytosolic low-molecular-weight markers. Under these conditions, the mitochondrial membrane potential significantly dropped. Based on this fact, the conclusion has been put forth that VDAC is converted into a locked state following the induction of a number of metabolic regulations [44]. This result provides strong support for a key role

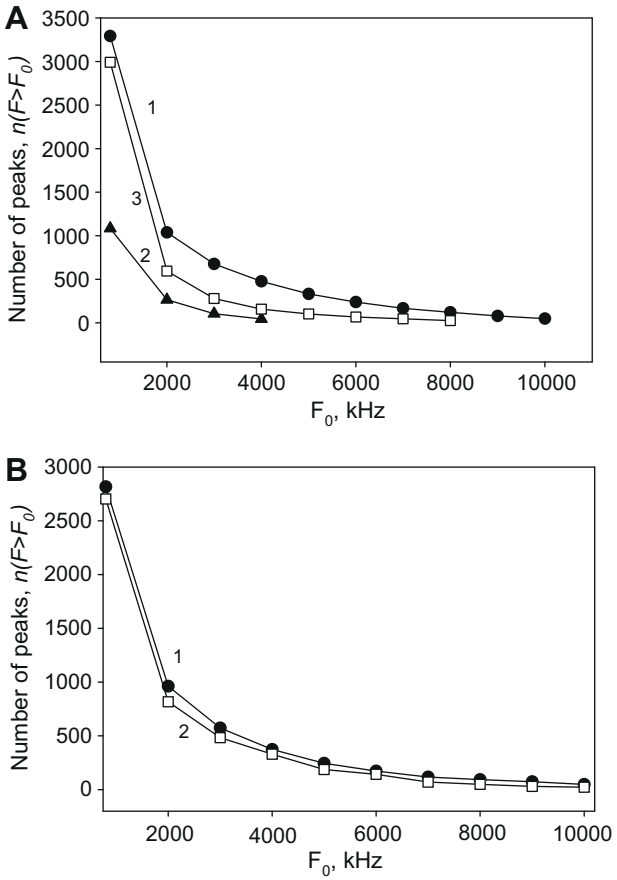

Fig. 5. (A) The effect of hexokinase on the plot of the number of FCS signal peaks ($n(F > F_0)$) of BODIPY-FL-ATP with amplitudes higher than the defined value (F_0) versus F_0 measured in mitochondrial suspension (0.04 mg/ml): (1) rat heart mitochondria supplemented with 2 μM rotenone, 25 nM BODIPY-FL-ATP; (2) mitochondria supplemented with 2 μM rotenone, 0.27 mg/ml hexokinase, 25 nM BODIPY-FL-ATP; and (3) mitochondria supplemented with 2 μM rotenone, 0.27 mg/ml hexokinase, 25 nM BODIPY-FL-ATP, 1 mM glucose 6-phosphate. (B) The effect of the peptide composed of the first 15 amino acids of hexokinase on the plot of the number of FCS signal peaks ($n(F > F_0)$) of BODIPY-FL-ATP with amplitudes higher than the defined value (F_0) versus F_0 measured in mitochondrial suspension (0.038 mg/ml): (1) rat heart mitochondria supplemented with 2 μM rotenone, 25 nM BODIPY-FL-ATP and (2) mitochondria supplemented with 2 μM rotenone, 0.07 mg/ml peptide, 25 nM BODIPY-FL-ATP.

of VDAC in a number of functionally critical metabolic regulatory pathways. It may also be helpful in further developing a strategy to reveal physiological regulation of VDAC conductance by different proteins or proteinaceous complexes.

Acknowledgements

We are grateful to Nataliya S. Egorova (Shemyakin-Ovchinnikov Institute of Bioorganic Chemistry, Russian Academy of Sciences, Moscow) for the synthesis of MIASHLLAYFFTELN-$CONH_2$ peptide and to Dr. Nikolay S. Melik-Nubarov at the Department of Polymer Sciences of the School of Chemistry at the Moscow State University for the synthesis of Koenig's polyanion. We are also thankful to Dr. Geert van den Bogaart (Max Planck Institute for Biophysical Chemistry, Göttingen) for improvement of software support for the PIA method. This work was supported by the RFBR grants 09-04-00890 (Y.N.A.) and 08-04-01667 (D.B.Z.).

References

[1] Colombini, M. (1979) A candidate for the permeability pathway of the outer mitochondrial membrane. Nature 279, 643–645.
[2] Colombini, M. (2004) VDAC: the channel at the interface between mitochondria and the cytosol. Mol. Cell. Biochem. 256–257, 107–115.
[3] Mannella, C.A., Forte, M. and Colombini, M. (1992) Toward the molecular structure of the mitochondrial channel. VDAC J. Bioenergy Biomembrane 24, 7–19.
[4] Mannella, C.A. and Kinnally, K.W. (2008) Reflections on VDAC as a voltage-gated channel and a mitochondrial regulator. J. Bioenergy Biomembrane 40, 149–155.
[5] Ujwal, R., Cascio, D., Colletier, J.P., Faham, S., Zhang, J., Toro, L., Ping, P. and Abramson, J. (2008) The crystal structure of mouse VDAC1 at 2.3 Å resolution reveals mechanistic insights into metabolite gating. Proc. Natl. Acad. Sci. USA 105, 17742–17747.
[6] Rostovtseva, T. and Colombini, M. (1996) ATP flux is controlled by a voltage-gated channel from the mitochondrial outer membrane. J. Biol. Chem. 271, 28006–28008.
[7] Rostovtseva, T. and Colombini, M. (1997) VDAC channels mediate and gate the flow of ATP: implications for the regulation of mitochondrial function. Biophys. J. 72, 1954–1962.
[8] Brdiczka, D.G., Zorov, D.B. and Sheu, S.S. (2006) Mitochondrial contact sites: their role in energy metabolism and apoptosis. Biochim. Biophys. Acta 1762, 148–163.
[9] Rostovtseva, T.K. and Bezrukov, S.M. (2008) VDAC regulation: role of cytosolic proteins and mitochondrial lipids. J. Bioenergy Biomembrane 40, 163–170.
[10] Wilson, J.E. (2003) Isozymes of mammalian hexokinase: structure, subcellular localization and metabolic function. J. Exp. Biol. 206, 2049–2057.
[11] Pastorino, J.G. and Hoek, J.B. (2008) Regulation of hexokinase binding to VDAC. J. Bioenergy Biomembrane 40, 171–182.
[12] Shoshan-Barmatz, V., Keinan, N. and Zaid, H. (2008) Uncovering the role of VDAC in the regulation of cell life and death. J. Bioenergy Biomembrane 40, 183–191.
[13] Shoshan-Barmatz, V., Zakar, M., Rosenthal, K. and Abu-Hamad, S. (2009) Key regions of VDAC1 functioning in apoptosis induction and regulation by hexokinase. Biochim. Biophys. Acta 1787, 421–430.
[14] Lemasters, J.J. and Holmuhamedov, E. (2006) Voltage-dependent anion channel (VDAC) as mitochondrial governator – thinking outside the box. Biochim. Biophys. Acta 1762, 181–190.
[15] Zorov, D.B., Isaev, N.K., Plotnikov, E.Y., Zorova, L.D., Stelmashook, E.V., Vasileva, A.K., Arkhangelskaya, A.A. and Khrjapenkova, T.G. (2007) The mitochondrion as janus bifrons. Biochemistry (Moscow) 72, 1115–1126.
[16] Robey, R.B. and Hay, N. (2006) Mitochondrial hexokinases, novel mediators of the antiapoptotic effects of growth factors and Akt. Oncogene 25, 4683–4696.
[17] Arzoine, L., Zilberberg, N., Ben Romano, R. and Shoshan-Barmatz, V. (2009) Voltage-dependent anion channel 1-based peptides interact with hexokinase to prevent its anti-apoptotic activity. J. Biol. Chem. 284, 3946–3955.
[18] Azoulay-Zohar, H., Israelson, A., Abu-Hamad, S. and Shoshan-Barmatz, V. (2004) In self-defence: hexokinase promotes voltage-dependent anion channel closure and prevents mitochondria-mediated apoptotic cell death. Biochem. J. 377, 347–355.
[19] Abu-Hamad, S., Zaid, H., Israelson, A., Nahon, E. and Shoshan-Barmatz, V. (2008) Hexokinase-I protection against apoptotic cell death is mediated via interaction with the voltage-dependent anion channel-1: mapping the site of binding. J. Biol. Chem. 283, 13482–13490.
[20] Armbruster, A., Hohn, C., Hermesdorf, A., Schumacher, K., Borsch, M. and Gruber, G. (2005) Evidence for major structural changes in subunit C of the vacuolar ATPase due to nucleotide binding. FEBS Lett. 579, 1961–1967.
[21] Hess, S.T., Huang, S., Heikal, A.A. and Webb, W.W. (2002) Biological and chemical applications of fluorescence correlation spectroscopy: a review. Biochemistry 41, 697–705.
[22] Chiantia, S., Ries, J. and Schwille, P. (2009) Fluorescence correlation spectroscopy in membrane structure elucidation. Biochim. Biophys. Acta 1788, 225–233.
[23] Perevoshchikova, I.V., Zorov, D.B. and Antonenko, Y.N. (2008) Peak intensity analysis as a method for estimation of fluorescent probe binding to artificial and natural nanoparticles: tetramethylrhodamine uptake by isolated mitochondria. Biochim. Biophys. Acta 1778, 2182–2190.
[24] Krichevsky, O. and Bonnet, G. (2002) Fluorescence correlation spectroscopy: the technique and its applications. Rep. Prog. Phys. 65, 251–297.
[25] van den Bogaart, G., Kusters, I., Velasquez, J., Mika, J.T., Krasnikov, V., Driessen, A.J. and Poolman, B. (2008) Dual-color fluorescence-burst analysis to study pore formation and protein–protein interactions. Methods 46, 123–130.
[26] Johnson, D. and Lardy, H. (1967) Isolation of liver or kidney mitochondria. Methods Enzymol. 10, 94–96.
[27] Smith, P.K., Krohn, R.I., Hermanson, G.T., Mallia, A.K., Gartner, F.H., Provenzano, M.D., Fujimoto, E.K., Goeke, N.M., Olson, B.J. and Klenk, D.C. (1985) Measurement of protein using bicinchoninic acid. Anal. Biochem. 150, 76–85.
[28] Zelenina, E.V., Avramova, L.V. and Goncharova, N.I. (1991) Preparation of hexokinase isoenzyme II with expressed adsorption properties. Biokhimiia 56, 1096–1103.
[29] Abu-Hamad, S., Sivan, S. and Shoshan-Barmatz, V. (2006) The expression level of the voltage-dependent anion channel controls life and death of the cell. Proc. Natl. Acad. Sci. USA 103, 5787–5792.
[30] Vignais, P.V. (1976) Molecular and physiological aspects of adenine nucleotide transport in mitochondria. Biochim. Biophys. Acta 456, 1–38.
[31] Colombini, M., Yeung, C.L., Tung, J. and Konig, T. (1987) The mitochondrial outer membrane channel, VDAC, is regulated by a synthetic polyanion. Biochim. Biophys. Acta 905, 279–286.
[32] Benz, R., Wojtczak, L., Bosch, W. and Brdiczka, D. (1988) Inhibition of adenine nucleotide transport through the mitochondrial porin by a synthetic polyanion. FEBS Lett. 231, 75–80.
[33] Pfaff, E., Klingenberg, M. and Heldt, H.W. (1965) Unspecific permeation and specific exchange of adenine nucleotides in liver mitochondria. Biochim. Biophys. Acta 104, 312–315.
[34] Winkler, H.H., Bygrave, F.L. and Lehninger, A.L. (1968) Characterization of the atractyloside-sensitive adenine nucleotide transport system in rat liver mitochondria. J. Biol. Chem. 243, 20–28.
[35] Florke, H., Thinnes, F.P., Winkelbach, H., Stadtmuller, U., Paetzold, G., Morys-Wortmann, C., Hesse, D., Sternbach, H., Zimmermann, B., Kaufmann-Kolle, P., Heiden, M., Karabinos, A., Reymann, S., Lalk, V.E. and Hilschmann, N. (1994) Channel active mammalian porin, purified from crude membrane fractions of human B lymphocytes and bovine skeletal muscle, reversibly binds adenosine triphosphate (ATP). Biol. Chem. Hoppe Seyler 375, 513–520.
[36] Yehezkel, G., Hadad, N., Zaid, H., Sivan, S. and Shoshan-Barmatz, V. (2006) Nucleotide-binding sites in the voltage-dependent anion channel: characterization and localization. J. Biol. Chem. 281, 5938–5946.
[37] Rostovtseva, T.K., Komarov, A., Bezrukov, S.M. and Colombini, M. (2002) Dynamics of nucleotides in VDAC channels: structure-specific noise generation. Biophys. J. 82, 193–205.
[38] Lee, A.C., Zizi, M. and Colombini, M. (1994) Beta-NADH decreases the permeability of the mitochondrial outer membrane to ADP by a factor of 6. J. Biol. Chem. 269, 30974–30980.
[39] Nakashima, R.A., Mangan, P.S., Colombini, M. and Pedersen, P.L. (1986) Hexokinase receptor complex in hepatoma mitochondria: evidence from N,N′-dicyclohexylcarbodiimide-labeling studies for the involvement of the pore-forming protein VDAC. Biochemistry 25, 1015–1021.
[40] Pastorino, J.G., Shulga, N. and Hoek, J.B. (2002) Mitochondrial binding of hexokinase II inhibits Bax-induced cytochrome *c* release and apoptosis. J. Biol. Chem. 277, 7610–7618.
[41] Beltrandelrio, H. and Wilson, J.E. (1992) Coordinated regulation of cerebral glycolytic and oxidative metabolism, mediated by mitochondrially bound hexokinase dependent on intramitochondrially generated ATP. Arch. Biochem. Biophys. 296, 667–677.
[42] Benz, R., Ed., (2004). Bacterial and Eukaryotic Porins: Structure, Function, Mechanism, Wiley-VCH, Weinheim.
[43] Kholodenko, B.N., Cascante, M. and Westerhoff, H.V. (1995) Control theory of metabolic channelling. Mol. Cell. Biochem. 143, 151–168.
[44] Lemasters, J.J. (2007) Modulation of mitochondrial membrane permeability in pathogenesis, autophagy and control of metabolism. J. Gastroenterol. Hepatol. 22 (Suppl. 1), S31–S37.